ISSN 1 746-7233, England, UK
World Journal of Modelling and Simulation
Vol. 13 (2017) No. 4, pp. 258-267

Study of loop antenna for ECG application using surface impedance concept

Khaoula Tayari[1*], Houda Werfelli[2], Mohamed Salah Karoui[3], Mondher Chaoui[4], Hamadi Ghariani[5], Mongi Lahiani[6]

Department of Electrical Engineering, LETI laboratory, National School of Engineering of Sfax, University of Sfax, Tunisia

(*Received June 28 2016, Accepted May 31 2017*)

Abstract. A rectangular loop antenna is proposed for monitoring of cardiac activity based on the concept of surface impedance at 433MHz. Relied on a parametric study and an adequate impedance matching, an optimal dimensional choice is made. The antenna is placed in the vicinity of the human thorax, which is considered to be a multi-layer structure: skin, fat and muscle. Each layer is similar to a characteristic impedance line. The lowest layer (muscle) is considered as a layer of variable thickness. Its impedance changes with progress to the surface. Then, a comparison with another model of the thorax is made.

Keywords: Cardiac activity, wireless electocardiogram, loop antenna, efficiency, surface impedance

1 Introduction

Cardiovascular diseases have been the most frequent cause of death. Today, however, it is essential to monitor cardiac patients not only in hospitals, but also in everyday life. So, because of the demographic change toward an aging population, "Personal Healthcare" scenarios are more applied[1, 11]. Electrocardiogram is the most important diagnostic methods to monitor heart function. For a long time, it has been known as a fast examination tool which can provide important signs to the status of the cardiac activity. Medical devices are intended to communicate wirelessly and to be used in the domestic environment[5, 12, 14]. It is often the tool of first choice in emergency situations.

Traditionally, ECG measures the electrical potential variations of specialized cells in contraction and those in automation. For electrocardiogram measurement conductive electrodes which are directly attached to the skin have been applied. Using contact gel, they provide a direct resistive contact to the patient. But, these electrodes have various disadvantages. They are not optimal for long-term use. In fact, as a result of drying of the contact gel and surface degradation of electrodes, the transfer resistance may change with time. Furthermore, metal allergies can cause skin irritations and may result in pressure necroses. On other hand, as a single-use item, they are rather expensive. Since 1967, a technique has been proposed: measuring potentials with isolated electrodes. It is already known through Richardson[15]. This capacitive measurement method is nowadays built into objects of everyday: like chairs[2], bathtubs[19], toilet seats[9] and incubators[8].

However, dry electrodes, which do not have the benefit of a conductive gel, require direct contact to the skin. In addition, they are limited to nonmedical and scientific applications like fitness monitoring owing its sensibility to the condition of skin and to the motion artifact. In other hand, patient often has to be immobilized. So an easier and less obtrusive method using wireless body sensor networks is needed as shown in Fig. 1.

The human body is not an ideal environment for the propagation of RF waves, especially at high frequencies. This dissipative environment will greatly reduce RF antenna performance especially in terms of pattern and radiation efficiency; a major portion of the power will be absorbed by the human tissues. RF antennas have large bandwidths, but they have low radiation efficiencies because of their environment. For this, we

* Corresponding author. *E-mail address*: Kaoula.tayari@gmail.com

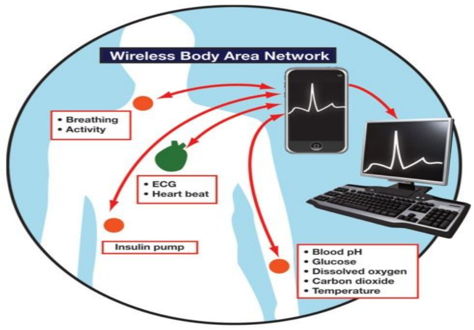

Fig. 1: Block diagram of wireless body sensor networks

have focused on loops, which have a near magnetic field independent of the dielectric properties of human tissues. Loop antennas have a very desirable property related to the robustness of the performance close to the human body. Indeed, the human body tends to have a large permittivity and low conductivity. The permittivity is the electric field tends to adjust the antenna response down in frequency. The conductivity of the body acts as a lossy material and absorbs energy from the antenna; which can seriously degrade the antenna efficiency. The human body affects the dipole antennas. Indeed, in the near field (very close to the antenna), the electric fields are particularly important. What is interesting is that the body is not really magnetic. Therefore, the magnetic fields do not really see the body as well and therefore is not affected as the electric fields. And because the antenna loop is somehow the "double" of the dipole, the magnetic fields are strong in the near field of the loop. These magnetic fields eventually give rise to the radiation from the antenna, and since they are somewhat immune to the human body. The loop antennas tend to be much more robust in terms of performance when placed near a human body. Accordingly, antennas in applications for medical telemetry are often loop antennas. This property makes them useful extremely antenna loop. The aim of this research is to use a new method of heartbeat detection that differs from conventional electrocardiograms; Detection based on the concept of surface impedance already defined in [17].

This paper presents, firstly, a detailed description of characteristics of loop antenna. Next, we will rely on a parametric study to make an optimal choice of the dimension of this loop. This loop will be used to detect the cardiac activity based on concept of surface impedance. Finally, a comparison of two different models of human thorax was made.

2 The loop antenna

2.1 Characteristics of loop antenna

Loop antennas are inexpensive and simple to build like dipoles and monopoles antenna . In addition, it was demonstrated that the loop antennas are more effective in equipment that is near the human body since their performance will not be degraded because of the low conductivity of the body [6, 16, 18]. The loop antennas take many different forms (circular, rectangular, triangular, elliptical, etc.), but their radiation patterns are largely independent of the shape of the loop. Indeed, all the loop antennas, having the same area, radiate energy in the same way; that is to say they have the same characteristics. The electrical size of the loop (circumference) determines its performance. Generally, loop antennas are classified on the basis of its circumference as electrically small if their circumference $\leq \lambda/10$ or electrically large if it is equal to λ.

The power density of a loop is given by:

$$\mathrm{p} = \frac{\mathrm{Z}_0}{2}[\frac{\mathrm{N}\pi\Delta s}{\mathrm{r}\lambda^2}]^2|I_0|^2\sin^2\theta. \quad (1)$$

With N represent the numbers of turns and $k = \omega\sqrt{\mu\varepsilon}$. The radiation level of a loop antenna is shown in the following expression:

$$U(\theta,\varphi)=\frac{Z_0}{2}[\frac{\mathrm{N}\pi\Delta s}{\lambda^2}]^2|I_0|^2\sin^2\theta. \tag{2}$$

The power radiated by the loop is given by:

$$\mathrm{P_{rad}}=\int_0^{2\pi}\int_0^{\pi}U(\theta,\varphi)\sin\theta \mathrm{d}\theta \mathrm{d}\varphi=\frac{1}{2}|I_0|^2\mathrm{R_{rad}}. \tag{3}$$

The directivity of the loop antenna is given by:

$$D(\theta,\varphi)=4\pi\frac{U(\theta,\varphi)}{P_{rad}}=1.5\sin^2\theta. \tag{4}$$

2.2 Equivalent electrical circuit of the loop antenna

The fields emitted by the short dipole and the loop antenna are dual quantities. Thereafter, the power emitted by the two antennas is the same. Therefore, they have the same equivalent circuits as shown in Fig. 2a.

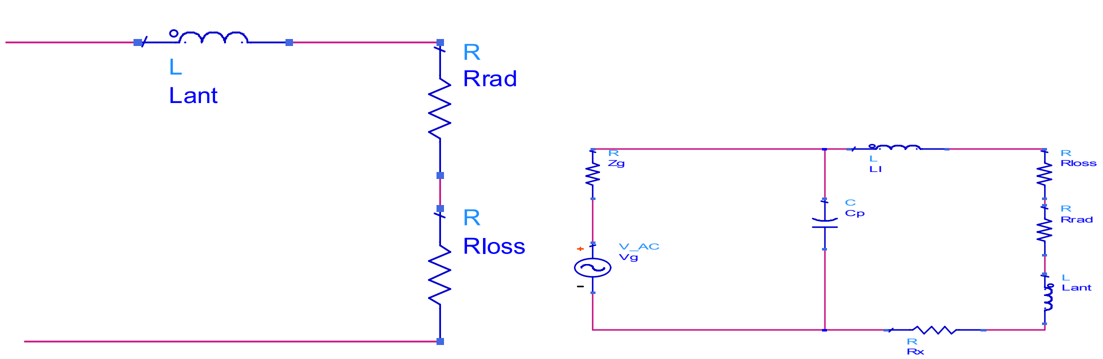

(a) A subfigure (b) A subfigure

Fig. 2: (a) Diagram of the equivalent loop antenna and (b) the equivalent schematic of the emission antenna

R_{rad} represents the resistance of radiation which is the energy radiated by the antenna. R_{loss} is the energy dissipated by Joule effect. While, L_{ant} is the inductance of the antenna. In general, radiation resistance of the small loop is smaller than that of the short dipole and its loss resistance is often greater than its radiation resistance [6]. Generally, we add an adjustable capacitor in parallel with the inductor to resonate the antenna at the operating frequency, increase its input impedance and suppress the inductive effect (Fig. 2b).

From this Figure, the input impedance Z_{in} is given by:

$$Z_{in}=(R_{rad}+R_{loss}+R_X)+j2\pi f(L_{ant}+L_l). \tag{5}$$

With: R_π : the ohmic losses resistance introduced by the capacitor;
l_1 : the inductance of the conductor.

Radiation resistance depends on the area of the loop and the frequency [20]. For a rectangular loop, it is given by [4]:

$$R_{rad}=31171\frac{N^2\Delta s^2}{\lambda^4}. \tag{6}$$

A loop antenna made for emission generally has one turn (N = 1). The loss resistance of the inductor for a rectangular loop is given by:

$$R_{loss} = \frac{Ncir}{2w'} \sqrt{\frac{\mu f \pi}{\sigma}}. \quad (7)$$

Knowing that, cir represents the antenna circumference, σ is the conductivity of copper (5.7.107 S/m) and b_2 (or w') represents the thickness of the copper. Taking into account the thickness of the copper, this expression becomes [3]:

$$R_{loss} = \frac{W + L}{b_1 + b_2} \sqrt{\frac{\mu f \pi}{\sigma}}. \quad (8)$$

The resistance ohmic loss which represents the additional losses introduced by the equivalent series resistance of the capacitor is expressed by:

$$R_X = \frac{2\pi f(L_l + L_{ant})}{Q} - R_{rad} - R_{loss}. \quad (9)$$

If " tol" represents the tolerance of the capacitor (%), so the quality factor Q is given by [4]:

$$Q = \frac{1}{\sqrt{1 + \frac{tol}{100} - l}}. \quad (10)$$

The third component in the model of figure 4 is the inductance Lant of the loop. It is given by the following equation [4, 13]:

$$L_{ant} = \frac{\mu}{2\pi} cir.Log(\frac{8s}{cir.w'}). \quad (11)$$

The inductance of the conductor is given by [3]:

$$L_l = \frac{\mu.A}{2a}. \quad (12)$$

With: $a = \sqrt{LW}$, $b = 0.35b_1 + 0.24b_2$ and $A = a_2$.

$\mu = \mu_0 = 410^{-7} kg.m.A^{-2}.s^{-2}$ is the permeability of vacuum and a represent the tube diameter. While N expresses the number of turns of the loop (generally N = 1).

3 Parametric study: selection of size

For circular loop antennas, we can only play on the radius. By cons, for rectangular loops, we can find a compromise between length and width. So the dimension can be reduced. There will be a compromise between size that should be as small as possible and the performance of our antenna. Our goal is to design a performing antenna loop around 433 MHz for medical telemetry particularly a wireless ECG in ISM (Industrial Scientific and Medical) band.

The quality of an antenna can be assessed according to their performance. The efficiency of an antenna is involved in the expression of the gain and thus the radiation pattern. So it is an important parameter. To do this, we must study the variation in the physical parameters of the loop and the selected frequency of operation. Note that to have maximum gain; it is necessary that the efficiency will be equal to 1.

$$\eta = \frac{R_{rad}}{R_{rad} + R_{loss}}. \quad (13)$$

Generally, the maximum value of the efficiency is determined by the dimensions of the antenna. So a wise choice of lengths and widths of the loop allows us to reach this maximum value or the worst case value of $\eta = 50\%$.

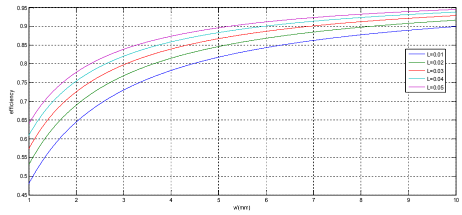

Fig. 3: Efficiency versus w' for different lengths L ($W = 30mm$)

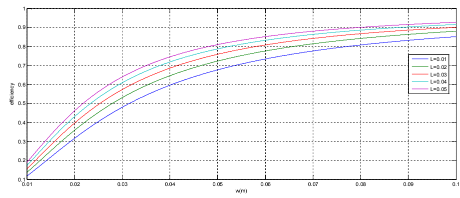

Fig. 4: Efficiency versus w' for different lengths L ($W = 30mm$)

First, we will set W=30mm and f=433MHz and we'll see the variation in performance depending on the antenna length L and the width of the copper w'. This variation is shown in Fig. 3.

It is clear from this figure that the efficiency increases with the length and width of the copper. For $L = 30mm$ and $w' = 1mm$, the efficiency is more than 50%. Therefore, in a first location, w' is fixed to 1 mm and we will see the effect of the width W on the antenna performance. The result is shown in the Fig. 4.

We can see in this figure that with $w' = 1mm$ and $W = 30mm$, we reaches 50% of efficiency than from a length L equal to 20mm. The performance will be important in increasing W. To see furthermore the performance of the loop, we'll fix w' to 1mm and W to 30mm and we'll see variation in performance depending on the frequency for different lengths L ranging from 10mm to 100 mm (Fig. 5).

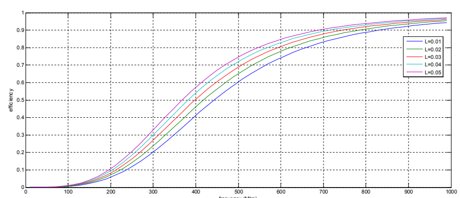

Fig. 5: Efficiency versus frequency for different L ($w' = 1mm$, W=30mm)

Note that for 433 MHz, choosing $w' = 1mm$ and $W = 30mm$, the efficiency exceeds 50% for a length greater than or equal to 20mm and to 68% for L of 50mm. It is advantageous to choose the highest value but since we're limited by the space on our work, it will be ideal for $L = 20mm$ corresponding to an efficiency of 50%.

4 Characteristics of the selected antenna

The proposed antenna consists of a rectangular loop (Fig. 6), printed on an $FR4_{e}poxy$ substrate ($\varepsilon_r = 4.4$, $tan\delta = 0.02$ and $h = 1.6mm$). Based on the parametric study, the loop is a conductor track with a width of 30mm and a length of 22mm. Its reflection coefficient is shown in Fig. 6.

As we shown in the last figure, the antenna resonates at 1.6 GHz. So we need to force the resonance at 433 MHz. For this, we have to make an adaptation of our antenna.

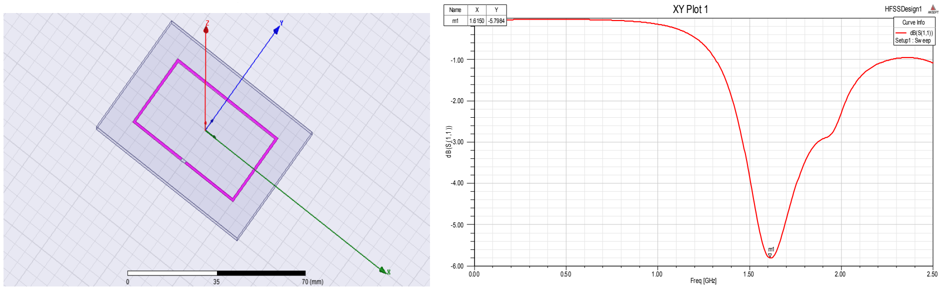

Fig. 6: Rectangular loop antenna in the air and reflection coefficient S_{11} of this loop

4.1 Adaptation of loop antenna

The antenna (Fig. 6) should be well adapted to the transmitter or receiver for maximum energy transfer with minimal losses. To satisfy these conditions, it is necessary that the input impedance Z_{in} of the antenna will be equal to the impedance of the source that is generally in the range of 50Ω. So, if the antenna is directly fed, the mismatch factor would be very broad. That is why we must add tuners to bring back this impedance to the desired value.

The mismatch factor mismatch that is desired as low as possible is given by:

$$\eta_{mismatch} = 1 - |\Gamma|^2 = \frac{4\frac{Z_{in}}{Z_0}}{(\frac{Z_{in}}{Z_0})^2 + 2(\frac{Z_{in}}{Z_0}) + 1} \tag{14}$$

With: Γ' is the reflection coefficient at the input of the antenna, Z_{in} is the antenna input impedance and Z0 is the impedance of the source.

Note that this is an amount that ranges from 0-1 with 1 being the ideal value. But this factor is different from antenna efficiency because it does not indicate the losses dissipated by Joule effect. The quality of the adaptation of the antenna input impedance isn't specified by the reflectivity or the mismatch factor but indicated by the return loss. This last indicates the quantity of the incident power that is not reflected or does not return from a load. It is given by:

$$R_L = 10Log_{10}(|\Gamma|^2) = 20Log_{10}(\frac{Z_{in} - Z_0}{Z_{in} + Z_0}). \tag{15}$$

The adaptation will be done using a small loop. This method comprises adding a small loop retaining the capacitor in parallel as shown in Fig. 7.

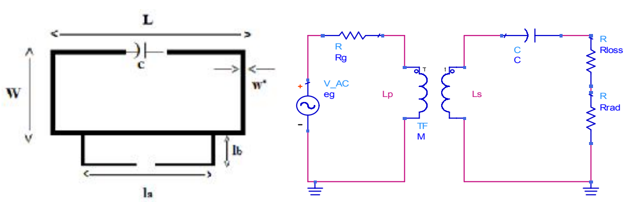

Fig. 7: Adaptation by adding a second loop and antenna tuning Scheme

The magnetic coupling between small loop and large loop leads to the action of a transformer where our loop is considered the secondary winding and the small antenna as the primary winding. The equivalent circuit is that of Fig. 7.

The capacitor C is used to compensate the inductance of the antenna. At resonance, it has the following expression:

$$C = \frac{1}{L_{ant}.\omega^2}. \tag{16}$$

Whereas the mutual inductance M, which allows reducing the impedance of our loop to that of the transmitter, will have the following formula:

$$M = \frac{\sqrt{R_g.R_{total}}}{\omega}. \tag{17}$$

With:

$$R_{total} = R_{loss} + R_{rad} \tag{18}$$

The mutual inductance can be expressed as a function of the dimensions of the antenna:

$$M = l_a \frac{\mu}{2\pi} Log(1 + \frac{4l_b}{w'}). \tag{19}$$

So l_a will be equal to:

$$l_a = \frac{\sqrt{R_g R_{total}}}{\mu f Log(1 + \frac{4l_b}{w'})}. \tag{20}$$

The loop antenna is shown in figure 8. Based on the parametric study, the loop has a width equal to $30mm$ and a length of $22mm$. The second loop has a width equal to $1mm$ and a length of $17mm$. The reflection coefficient S_{11} of the loop is equal to 15.07 dB (Fig. 8). The gain and the efficiency of this antenna are shown in Fig. 9.

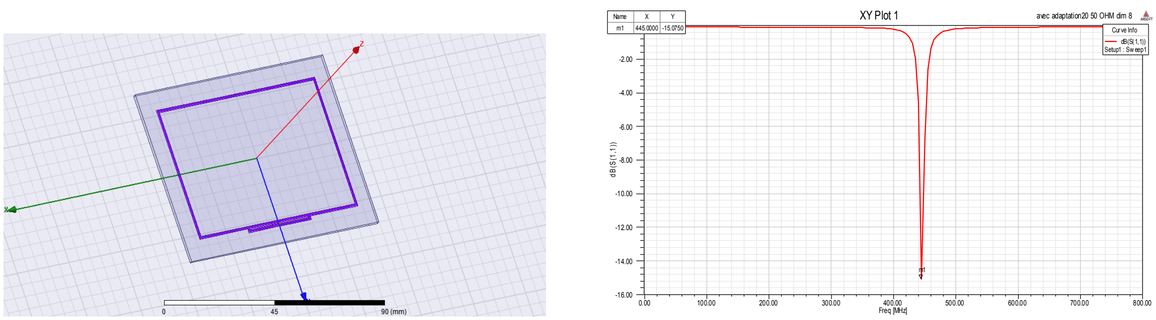

Fig. 8: The loop antenna and the reflection coefficient S_{11} of the adaptive loop antenna

Fig. 8: The loop antenna and the reflection coefficient S_{11} of the adaptive loop antenna

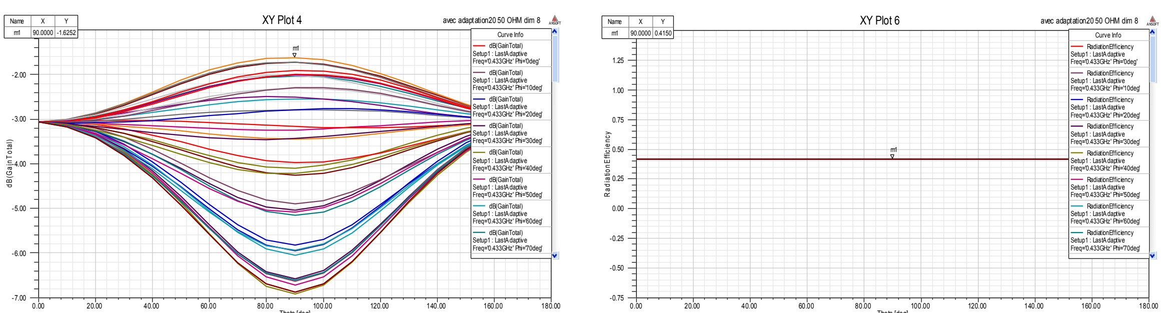

Fig. 9: Gain and efficiency of the loop antenna

4.2 Using of loop antenna for detection of cardiac activity based on the concept of surface impedance

The normal electrical conduction in the heart allows the impulse that is generated by the senatorial node to spread. The latter stimulates the heart muscle (myocardium). So it causes contraction and relaxation of the muscle. This leads, subsequently, variation of its thickness. As the antenna is intended for application in the vicinity of human body simulation was performed using a model of human tissue simplified in three layers (skin, fat, muscle) as it is shown in Fig. 10. This model was well detailed in [10].

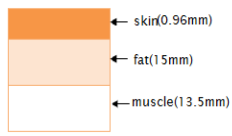

Fig. 10: Model of human thorax

Each layer is similar to a characteristic impedance line. The lowest layer (muscle) is considered as a variable thickness layer. And the surface of the last one (skin) is regarded as a wave transmission medium. Therefore, the impedance of the muscle will be transformed as and as one progresses to surface. The purpose of this part is to see the influence of the variation in thickness of the lower layer on the surface impedance which will be reflected in a variation of the characteristics of antenna. The lowest layer varied from 24mm to 38mm. The antenna is placed close to the tissue (1 cm). The characteristics of the loop are shown in Figure 11. The coefficient of reflection S_{11} varied from -11.7 dB to -7.3 dB (Fig. 11). Else the gain varied with thickness of lowest layer as shown in Fig. 11.

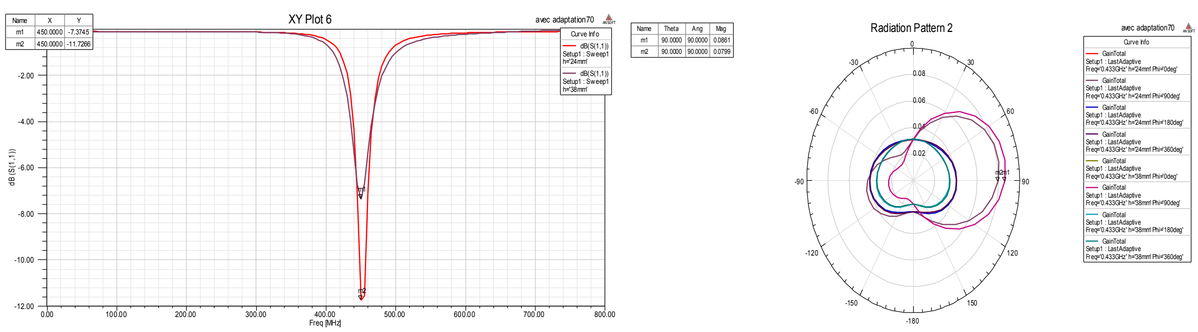

Fig. 11: Model of human thorax

As shown in the preceding figures, the antenna is sensitive to changes in the impedance of the surface of the chosen model. So we can use this new method to the monitoring of cardiac activity. Next we will compare this method with other reported in literature.

4.3 Monitoring of cardiac activity based on the variation of the heart volume

On the basis of changes in dimension of the cavity, wall thickness over time and their peak rate change as specified in [7], the total core height (in millimeters) during the systole and diastole is obtained for a complete cardiac cycle of 0.8 seconds as shown in Tab. 1.

We will use the same adaptive rectangular loop antenna with the same human model (skin, fat and muscle) but with fixed thicknesses (12a) adding the heart (sphere). This time we will be based on the volume change of heart as shown in Tab. 1.

As shown in latter curves, the antenna is insensitive to variations in the heart dimension. Its characteristics remain unchanged.

Table 1: Instant dimensions of human heart

Cardiac activity	Time (s)	Heart dimension (mm)
End of diastole and systole early	0	111.4
Systole	0.1	103.7
	0.2	102.3
	0.3	100.4
End of systole and diastole early	0.4	102.8
	0.5	106.3
	0.6	107.8
Diastole	0.7	108.8
End of diastole	0.8	111.4

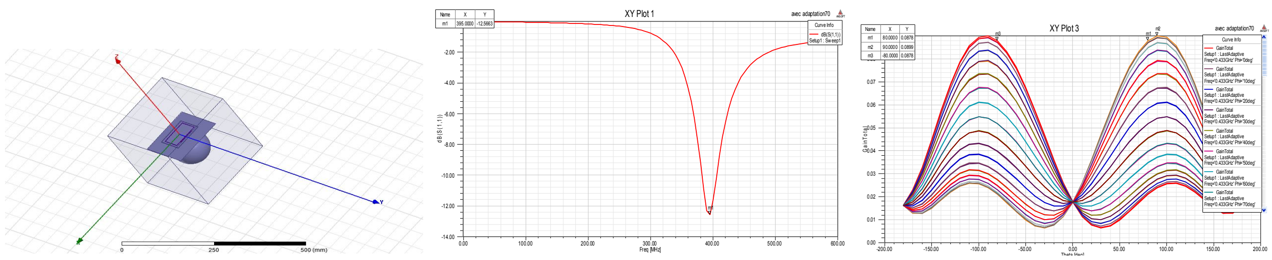

(a) (b) (c)

Fig. 12: (a) A new model based on four layers (skin, fat, muscle and heart), Characteristics of the loop antenna for a heart dimension equal to 100.4 mm: (b) Reflection coefficient S_{11} and (c) Gain

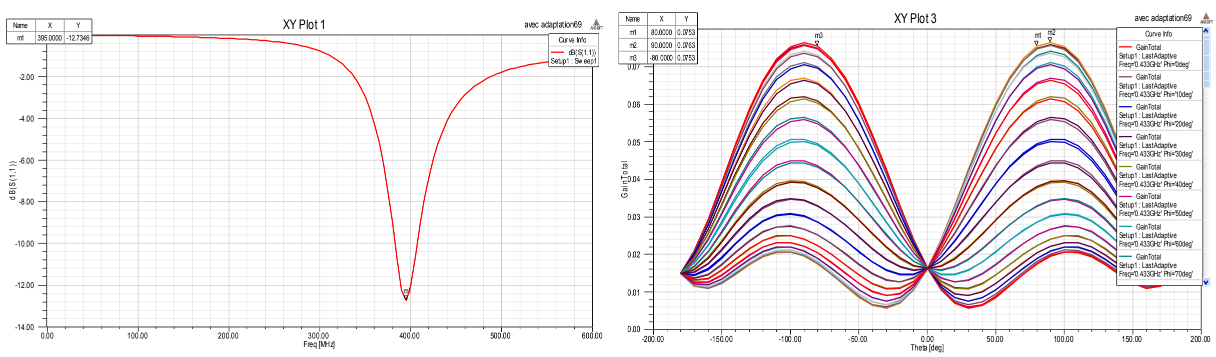

(a) (b)

Fig. 13: Characteristics of the loop antenna for a heart dimension equal to 111.4 mm: (a) Reflection coefficient S_{11} and (b) Gain

5 Conclusion

Biological tissues are considered as multilayer structures. We used in this paper a three-layer model: skin(0.96mm), fat(15mm) and muscle(13.5mm). This structure can be linked to a cascading line model in which each tissue has its own characteristics. The impedance of the first layer will be transformed as soon as one moves towards the surface. This structure has been studied using a magnetic coupling between a primary rectangular loop (1mmx17mmx1mm) and a secondary one (22mm $\times$ 30mm $\times$ 1mm). So an attempt has been made to make a judicious choice of the type of antenna which should have desirable properties related to robustness and performance in the vicinity of the human body. Next, we have demonstrated that the variation of the surface impedance has a significant influence on the characteristics of the rectangular loop (reflection coefficient from -11.7 dB to -7.3 dB and gain). But when we used the second model taking the heart as a sphere and playing on its volume, the loop antenna was not sensitive to the variation in the size of the heart between the systole and the diastole phase. We can therefore conclude that we can use the concept of surface impedance to monitor wirelessly heart activity. Future work will focus on studying the interaction between the loop antenna and the human body and then designing a complete ECG system complying with our goals (miniature, low power consumption and mobility).

References

[1] Dynamics of a cardiovascular model obtaining measurable pulsatile pressure output.

[2] T. W. A. Schommartz, B. Eilebrecht. Advances in modern capacitive ecg systems for continuous cardiovascular monitoring. *Acta Polytechnica*, 2011, **51**(5).

[3] N. V. ASA. Small loop antennas, 2000. NAN400-03, Revision: 1.2.

[4] F. Callais. Loop antennas; wave short; formulas and application to an antenna reception, 2006. HB9BLF CH-2046 Fontaines.

[5] G. Ghassabi, M. Kahrom. Optimization of heat transfer enhancement of a domestic gas burner based on pareto genetic algorithm: experimental and numirecal approach. *International Journal of Engineering transactions A: Basics*, **26**.

[6] J.V.Niekerk. Matching small loop antennas to rfpic device, 2002. Microchip Technologie Inc.

[7] M. S. K. N. Sahu, C. D. Naidu. Study of rf signal attenuation of human heart. *Hindawi Publishing Corporation Journal of Engineering*, 2015.

[8] T. Kato, A. Ueno, K. et al. An application of capacitive electrode for detecting electrocardiogram of neonates and infants. *Conf Proc IEEE Eng Med Biol Soc.*, 2006, **1**: 916–919.

[9] K. K. Kim, Y. K. Lim, K. S. Park. The electrically non-contacting ecg measurement on the toilet seat using the capacitively-coupled insulated electrodes. **in:** *International Conference of the IEEE Engineering in Medicine & Biology Society*, 2004, 2375.

[10] M. e. a. K.Tayari, H.Werfelli. Modeling of the thorax of human body at 433 mhz. *ATSIP*, 2016, 21–24.

[11] S. Mahmoudzadeh, H. Mojallali, N. Pourjafari. An optimized pid for capsubots using modified chaotic genetic algorithm. *International Journal of Engineering (1025-2495)*, 2014, **27**(9).

[12] S. Mukherjee, R. M. Aarts, R. Roovers. Amiware hardware technology drivers of ambient intelligence. *Philips Research*, 2006, **5**.

[13] Nikolova. Loop antennas, 2014.

[14] R. A. P. Raghavendran1. Improved qos in wireless sensor networks deployed for health monitoring of plant operators. *World Journal of Modelling and Simulation*, **10**.

[15] P. C. Richardson. **in:** *The Insulated Electrode*, Proceedings of the 20th Annual Conference on Engineering in Medicine and Biology, Boston, MA (USA), 1967, 157.

[16] Y. Saito, I. Nagano, H. Haruki. A novel loop antenna for a wristwatch phone. *Ieice Transactions on Communications*, 2001, **E84B**(5): 1423–1430.

[17] K. Tayari, M. Chaoui, H. Ghariani. Influence of the cardiac activity on the surface impedance of a multilayer model. **in:** *International Conference on Advanced Technologies for Signal and Image Processing*, 2014, 340–345.

[18] Y. K. Y Kim, H Morishita. A folded loop antenna system for handsets developed and based on the advanced design concept. *IEICE Trans.Commum*, 2001, **E84-B**(9).

[19] K. L. Yong, K. K. Kim, K. S. Park. The ecg measurement in the bathtub using the insulated electrodes. **in:** *Engineering in Medicine and Biology Society, 2004. Iembs '04. International Conference of the IEEE*, 2005, 2383–2385.

[20] R. J. Zavrel. How antenna aperture concerne to gain and directivity, 2004. W7SX, quarterly QEX May / June.